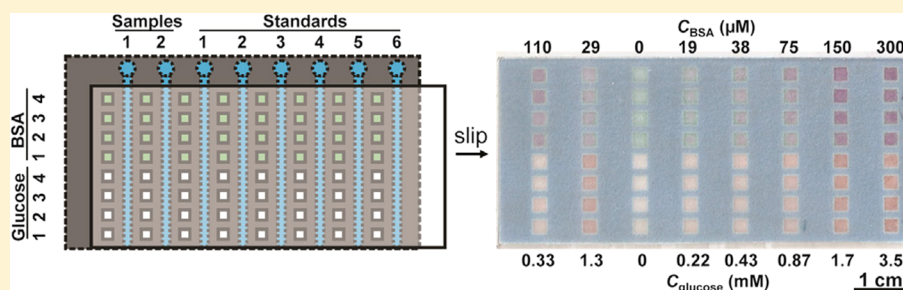


## Paper-Based SlipPAD for High-Throughput Chemical Sensing

Hong Liu,<sup>†</sup> Xiang Li, and Richard M. Crooks\*

Department of Chemistry and Biochemistry, The University of Texas at Austin, 105 East 24th Street, Stop A5300, Austin, Texas 78712-1224, United States

## Supporting Information



**ABSTRACT:** We report a paper analytical device (PAD) that is based on the SlipChip concept. This SlipPAD enables robust, high-throughput, multiplexed sensing while maintaining the extreme simplicity of paper-based analysis. The SlipPAD is comprised of two wax-patterned paper fluidic layers. By slipping one layer relative to the other, solutions wick simultaneously into a large array of sensing reservoirs or sequentially into a large array of channels to carry out homogeneous or heterogeneous assays, respectively. The applicability of the device to high-throughput multiplex chemical analysis is demonstrated by colorimetric and fluorescent assays.

Here we report a paper analytical device (PAD)<sup>1</sup> that is based on the SlipChip<sup>2,3</sup> concept. This SlipPAD enables robust, high-throughput, homogeneous and heterogeneous sensing while maintaining the extreme simplicity of paper-based analysis. The basic principle of the SlipPAD is illustrated in Figure 1. The device is comprised of two paper fluidic layers that are patterned using wax printing onto chromatographic paper.<sup>4–6</sup> The two paper layers are attached to rigid substrates, and they are in sufficiently close contact that the wax prevents leakage of liquids between channels and reservoirs, while simultaneously reducing friction between the layers to ensure smooth sliding operation. When one layer is slipped, fluidic contacts are opened or closed between the two layers. In analogy to previously reported glass SlipChips,<sup>2</sup> this provides a means to simultaneously load large arrays of reaction chambers with precise aliquots of samples and reagents, time reactions, and introduce washing steps for assays. All of these functions are highly developed for plastic and glass chips, but they still represent major hurdles for PAD-based assays.<sup>7–10</sup> Moreover, we demonstrate that this device enables high-throughput chemical sensing, on-chip calibration, and introduction of both preloaded and user-loaded reagents. Hence, it represents a significant advance compared to the present state of the art in the field of paper fluidics.<sup>11</sup>

The SlipPAD is important for the following specific reasons. First, the current version of the SlipPAD has the form factor of a business card, and it enables simultaneous delivery of solution into 285 reservoirs having volumes of ~180 nL with no observable cross contamination. This means that it could be used to replace plastic microtiter plates for some assays, thereby

reducing cost on both the front and back end (i.e., biohazard disposal). Second, fabrication is fast and inexpensive: just a \$600 U.S. wax printer and a hot plate are required. In the lab, a single individual can produce ~200 devices per hour at a cost of <\$1 U.S. each, and these values would likely dramatically increase and decrease, respectively, at production scale. This means that the SlipPAD technology is immediately accessible to any laboratory with access to a wax printer. Importantly, prior to this report, the SlipPAD technology has only been demonstrated for glass devices, which require much more sophisticated fabrication. Third, as we show here, the large number of reservoirs on the SlipPAD provide a means for on-chip calibration and multiple, simultaneous, replicate assays for improved diagnostic reliability. Fourth, the device is naturally amenable to both colorimetric (including naked eye) and fluorescent assays.

The SlipChip and its underlying operational principles have been reported by Ismagilov and co-workers.<sup>2,12–20</sup> In 2009, they introduced the SlipChip for multiplexed manipulation of liquids on the nanoliter scale without the need for pumps or valves.<sup>12</sup> Several interesting applications, including protein crystallization,<sup>13,14</sup> digital PCR,<sup>15–17</sup> and immunoassays<sup>18</sup> have been reported. The SlipChip is comprised of two glass plates having photolithographically patterned microchannels and microwells. Silanization and nanopatterning to increase contact angles of liquid on the glass, as well as a fluorocarbon lubricant,

Received: March 22, 2013

Accepted: April 8, 2013

Published: April 15, 2013

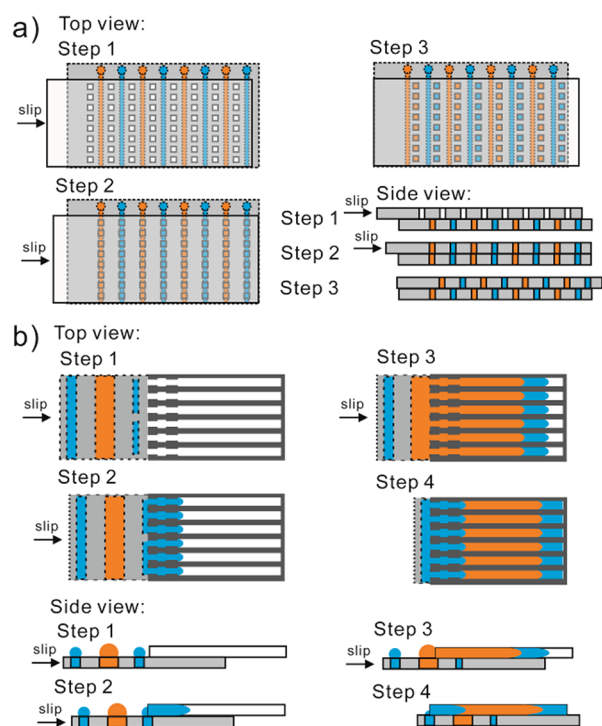


**Figure 1.** Schematic illustration showing the operating principle of the SlipPAD for (a) parallel and (b) sequential fluidic manipulation. Both devices are comprised of two layers. The bottom layers, and the fluidic channels and reservoirs patterned therein, are highlighted by black dashed lines in the top views.

are required to avoid cross contamination of liquids and to ensure smooth movement of the two plates relative to one another. The SlipChip is a very promising technology for manipulating small volumes of solution and will lead to useful applications. The innovations described here provide significant simplifications over the existing technology that will provide a more desirable design for certain types of point-of-care applications.<sup>21</sup> However, like all paper-based technologies these advances come at the expense of reproducibility, limit of detection, and sensitivity, which of course are the advantages of glass and plastic microdevices.

## EXPERIMENTAL SECTION

**Chemicals and Materials.** The colorimetric glucose assay kit and the fluorescent BSA assay kit were purchased from Sigma-Aldrich. The colorimetric BSA assay kit was purchased from Fisher Scientific. Erioglaucine disodium salt was purchased from Acros Organics. Tartrazine were obtained from MP Biomedicals (Solon, OH). Biotin-labeled Au nanoparticles were purchased from Cytodiagnosics (Burlington, Canada). Streptavidin-labeled polystyrene microbeads ( $\sim 10 \mu\text{m}$  in diameter) were purchased from Spherotech (Lake Forest, IL). Whatman grade 1 chromatographic paper and Corning glass slides (1 mm thick, 75 mm  $\times$  50 mm) were obtained from Fisher Scientific. Elmer's all-purpose glue stick was purchased from Office Depot. All solutions were prepared with deionized water (18.0 M $\Omega$  cm, Milli-Q Gradient System, Millipore). All reagents were used as received without further purification.

**Experimental Procedures.** The patterning of paper is based on a slight modification of a wax printing procedure reported previously.<sup>6</sup> Briefly, a Xerox 8570DN inkjet printer

was used to print wax-based solid ink on Whatman chromatography paper. The paper was then placed on a hot plate with the wax side up for 45 s at 120  $^{\circ}\text{C}$  and then cooled to 20  $^{\circ}\text{C}$ .

For preparing the reagent solution for the colorimetric BSA assay, 30  $\mu\text{L}$  of 4%  $\text{CuSO}_4$  solution was mixed with 90  $\mu\text{L}$  of bicinchoninic acid solution from the assay kit. For the colorimetric glucose assay and the fluorescent BSA assay, all the reagents are from the assay kits and are prepared according to the instructions of the kit provider. Next, 2.0  $\mu\text{L}$  aliquots of the reagent solutions were dropcast onto the reservoir ( $\sim 2 \text{ mm} \times 2 \text{ mm}$ ) patterned on the chromatography paper. The solution was allowed to dry at 20  $^{\circ}\text{C}$  under nitrogen. The paper fluidic layers were then attached to glass slides using the glue stick. For the user-loaded SlipPAD, 25  $\mu\text{L}$  aliquots of assay reagents were delivered into reservoirs on the top layer via channels on the bottom layer. After drying at 20  $^{\circ}\text{C}$  under nitrogen, the top layer was assembled with another bottom layer to inject samples and standard solutions.

An office scanner (HP C6180) was used to obtain optical images of the paper fluidic device. Fluorescent scanning of the paper fluidic device was carried out using a Typhoon Trio fluorescent imager (GE Healthcare, Piscataway, NJ). Each paper layer was scanned at a lateral resolution of 100  $\mu\text{m}$ , using a 532 nm, 20 mW solid-state laser as the light source and a 640 nm emission filter.

## RESULTS AND DISCUSSION

Figure 2a is a photograph of a simple, two-level SlipPAD. The 285 reservoirs, which have lateral dimensions of 1 mm  $\times$  1 mm and volumes of  $\sim 180 \text{ nL}$ , were printed onto Whatman grade 1 chromatography paper using a Xerox model 8570DN wax printer. The basic operation of the device is illustrated by introducing 30  $\mu\text{L}$  aliquots of 0.010 M PBS (pH 7.4) containing either 1.0 mM erioglaucine (blue) or 1.0 mM tartrazine (yellow) at the inlets of the channels on the bottom layer (red arrow). This fills the channels. Next, the top layer is slipped to the left so that the solutions wick into all of 285 reservoirs in the top layer. The movie in the Supporting Information shows that all the reservoirs are filled within 2 s. Slipping and the aligning the two layers can be carried out manually (movie in the Supporting Information), or the SlipPAD can be sandwiched within a simple plastic support to enhance reproducibility (Figure S2 in the Supporting Information). The top paper layer of the device is then scanned using an office scanner (HP C6180). As shown in Figure 2b, the colored solutions are delivered to the designated reservoirs without cross contamination.

To demonstrate the applicability of the device for high-throughput multiplexed homogeneous sensing, a SlipPAD having 64 detection reservoirs was fabricated by wax printing. As shown in Figure 2c, cyan-colored wax (rather than black) was used to improve contrast for the colorimetric assay. Each reservoir in the upper half of the array was preloaded with a dried colorimetric indicator for detection of bovine serum albumin (BSA), and each reservoir in the bottom half was preloaded with a dried indicator for the presence of glucose. The detection of BSA is based on a bicinchoninic acid assay, in which peptide bonds present in BSA reduce  $\text{Cu}^{2+}$  to  $\text{Cu}^+$  resulting in a purple-colored chelate complex.<sup>22</sup> The detection of glucose is based on a two-step reaction: (1) glucose oxidase-catalyzed oxidation of glucose to yield  $\text{H}_2\text{O}_2$  and (2) horseradish peroxidase-catalyzed oxidation of *o*-dianisidine by

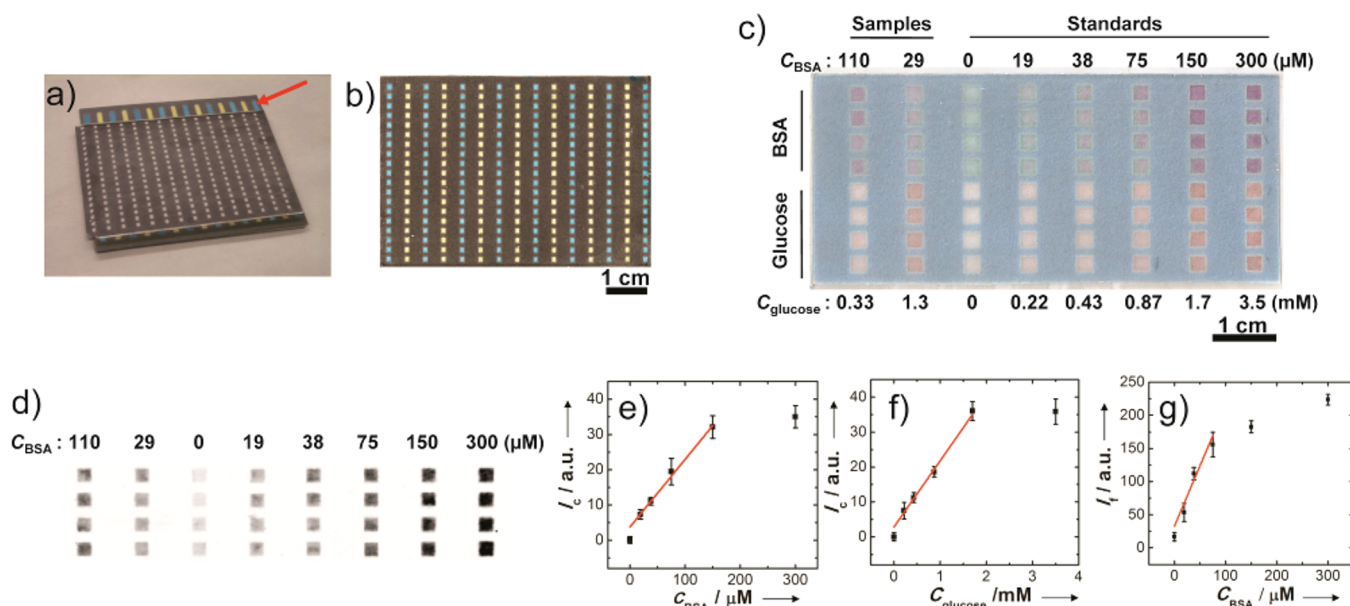


**Figure 2.** (a) A photograph of a SlipPAD comprised of two paper fluidic layers patterned by printing black-colored wax. The paper layers were attached to glass slides (1 mm thick, 7.5 cm  $\times$  5.0 cm) using glue to ensure uniform contact and hence eliminate leaking. Aliquots (30  $\mu\text{L}$ ) of 0.010 M PBS solution (pH 7.4) containing either 1.0 mM erioglaucine (blue) or 1.0 mM tartrazine (yellow) were loaded at the inlets of channels (1.5 mm wide, marked with a red arrow) on the bottom layer. (b) The top layer after the slipping step. In total, 285 reservoirs on this layer were simultaneously filled with the colored solutions. Each of the reservoirs was 1 mm square and 180  $\mu\text{m}$  in depth, which is equivalent to a geometric volume of 180 nL. Note that this value is an upper bound and does not take into account the enclosed volume of cellulose. (c) Scanometric image of the top layer of the SlipPAD showing the detection reservoirs (2 mm square) after completion of the assay. The concentrations of BSA and glucose in each standard or sample are indicated. A color change from green to purple indicates the presence of BSA, and a change from colorless to brown indicates the presence of glucose. (d) Fluorescence image of the top layer of the device showing the detection reservoirs (2 mm square) for the fluorescent BSA assay. (e and f) Plots of color intensity measured from part c as a function of (e) BSA and (f) glucose concentration. The red lines are linear fits from 19 to 150  $\mu\text{M}$  for BSA and from 0.22 to 1.7 mM for glucose. The error bars represent standard deviations for four replicate assays. For both parts c and d, the color intensities were normalized by subtracting the intensity of the sample containing no BSA or glucose. (g) A plot of fluorescence intensity measured in part d as a function of BSA concentration. The red line is the linear fit from 19 to 75  $\mu\text{M}$ . The error bars represent standard deviations for four replicate assays.

$\text{H}_2\text{O}_2$  to yield a brown-colored compound.<sup>23</sup> More details about these assays are provided in the Supporting Information. For both assays, 30  $\mu\text{L}$  aliquots of standard solutions containing BSA and glucose at known concentrations were injected into the six channels on the right (Figure 2c). Likewise, 30  $\mu\text{L}$  aliquots of samples having intermediate concentrations were injected into the two channels on the left. The top layer was then slipped to the left so that the standards and samples in the channels wicked into the designated reservoirs to react with the preloaded assay reagents. Finally, the top layer was slipped further to the left to fully isolate the top reservoirs from the channels. The colors, which are related to the concentrations of the analytes, were developed within 10 min. A single SlipPAD enables four simultaneous replicate assays for both the standards and the samples.

As shown in Figure 2c, the intensity of the color change from green to purple is correlated to the BSA concentration, and the intensity of the color change from colorless to brown is correlated to the glucose concentration. Importantly, no cross contamination between the BSA and glucose assays is observed. The color changes of the standard solutions provide a guide for naked-eye, semiquantification of the concentrations of BSA and glucose in the samples. For example, the purple color in the reservoirs containing sample 1 (110  $\mu\text{M}$  BSA) is more intense than that of standard 4 containing 75  $\mu\text{M}$  BSA but less intense than that of standard 5 containing 150  $\mu\text{M}$  BSA, indicating the concentration of BSA in sample 1 is between 75  $\mu\text{M}$  and 150  $\mu\text{M}$ . To better quantify these results, the image in Figure 2c was

imported into Adobe Photoshop CS2, and the color intensity was obtained from a histogram of each reservoir. The color intensities were then linearly correlated to the concentrations of BSA and glucose using the calibration curves in parts e and f of Figure 2, respectively. The limits of detection, defined as 3 times the standard deviation of the sample containing no BSA or glucose divided by the slope of the calibration curve, are 15  $\mu\text{M}$  for BSA and 0.19 mM for glucose. The intensities of the four replicate assays are quite reproducible (relative standard deviation <3%). On the basis of the calibration curves, the concentrations of BSA and glucose in sample 1 are determined to be 100  $\mu\text{M}$  and 0.30 mM, respectively, and the concentrations of BSA and glucose in sample 2 are 26  $\mu\text{M}$  and 1.4 mM, respectively. The deviations from the actual concentrations are all <12%. One final point. Although the data shown in Figure 2c were obtained using a scanner, the assay can also be carried out on a semiquantitative basis by simple visual inspection.

In the example discussed above, the colorimetric reagents were manually loaded into each reservoir using a pipet. However, for larger arrays or large numbers of SlipPADs, this approach is untenable. To address this problem, Ismagilov and his colleagues invented a SlipChip that can easily be loaded with reagents by an end user.<sup>13</sup> In that case, multiple reservoirs were connected by a channel so that all of them were filled with reagents using a single injection. Here we show that this same function is achievable in the SlipPAD format. This example also demonstrates that in addition to colorimetry, the SlipPAD can

also be interrogated using fluorescence. The assay is based on the dye epicocconone, which exhibits enhanced fluorescence in the presence of BSA.<sup>23</sup> As shown in Figure S1 in the Supporting Information, 25  $\mu\text{L}$  aliquots of assay reagents were delivered into the reservoirs of the top layer through the channels on the bottom layer. After drying, the top layer was removed and connected to a second bottom layer for injection of sample and standard solutions. Note that switching layers is very easy and highly reproducible. Subsequent operations of this SlipPAD are the same as for the colorimetric assay, except that a fluorescence scanner was used to obtain the images shown in Figure 2d. The key result is that the fluorescence intensity is linearly correlated to the concentration of BSA from 19 to 75  $\mu\text{M}$  (Figure 2g) and the detection limit is 10  $\mu\text{M}$ . The concentrations of BSA for the samples were found to be 100 and 31  $\mu\text{M}$ . The deviations from the actual concentrations are within 9%.

For many bioassays, methods relying on a bound probe are more convenient than the sort of homogeneous methods discussed thus far. However, heterogeneous assays are difficult to implement in paper-based devices because they require multiple timed steps: binding of the target, washing, and chemical amplification. To demonstrate the applicability of the SlipPAD for high-throughput heterogeneous sensing, a different type of SlipPAD was fabricated (the design is shown in Figure 1b). As shown in Figure 3a, three solutions loaded on the

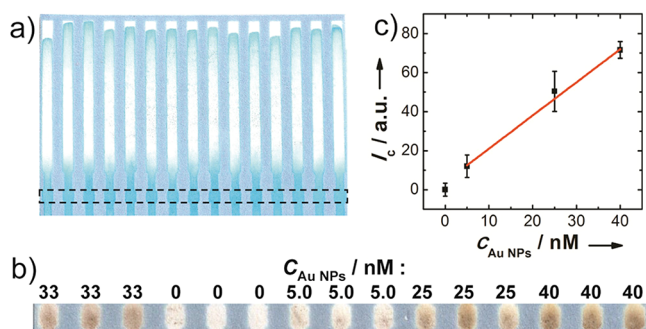


**Figure 3.** (a) Top layer of a SlipPAD (Figure 1b) having 15 fluidic channels after sequential injections of 1.0 mM erioglaucline (blue), 0.010 M PBS buffer (pH 7.4) containing 0.05% tween-20 (colorless), and 1.0 mM erioglaucline (blue) from the bottom layer. The device was also used to carry out 15 parallel colorimetric heterogeneous assays. The detection zones are highlighted by dashed black lines. (b) Scanometric image of the top layer of the SlipPAD showing the detection zones after completion of the sensing assay. The detection zones were preloaded with 2.0  $\mu\text{L}$  of 0.5% w/v streptavidin-labeled microbeads ( $\sim 10 \mu\text{m}$  in diameter). A volume of 3.0  $\mu\text{L}$  of biotin-labeled Au NPs, 10  $\mu\text{L}$  of PBS buffer (pH 7.4) containing 0.05% tween-20 (washing buffer), and 3.0  $\mu\text{L}$  of Ag enhancement solution were sequentially injected into the channel by slipping the device (Figure 1b). (c) A plot of color intensity as a function of Au NP concentration. The red line is a linear fit from 5 to 40 nM. The error bars represent standard deviations for three replicate assays. The color intensities were normalized by subtracting the intensity of the sample containing no Au NP.

bottom layer (100  $\mu\text{L}$  of 1.0 mM erioglaucline, 300  $\mu\text{L}$  of 0.010 M PBS buffer (pH 7.4) containing 0.05% tween-20 (colorless), and 100  $\mu\text{L}$  of 1.0 mM erioglaucline) were sequentially injected into the 15 channels on the top layer with acceptable reproducibility. Using the SlipPAD, heterogeneous detection of streptavidin–biotin binding was carried out as follows. First, 3.0  $\mu\text{L}$  of 0.5% w/v streptavidin-labeled microbeads ( $\sim 10 \mu\text{m}$

in diameter) were dropcast in each of the detection zones (highlighted by the dashed black lines in Figure 3a) and allowed to dry. Second, 3.0  $\mu\text{L}$  of biotin-labeled Au nanoparticles (NPs) were injected into each channel so that the Au NPs were captured by the entrapped microbeads due to streptavidin–biotin binding.<sup>24</sup> Third, 10  $\mu\text{L}$  of PBS buffer (pH 7.4) containing 0.05% tween-20 (washing buffer) was introduced into each channel to remove nonspecifically adsorbed Au NPs. Finally, 3.0  $\mu\text{L}$  of Ag enhancement solution was injected into the channel. This amplifies the presence of the Au NPs because the latter catalyze electroless Ag deposition. As shown in Figure 3b, four standards and one sample were assayed simultaneously. The intensity of the brown (Ag) color increases with increasing concentration of Au NPs, and the color intensity is linearly correlated to the concentration of the target in the range from 5 to 40 nM (Figure 3c). The detection limit is 4.8 nM. From the calibration curve, the concentration of Au NPs in the sample was determined to be 35 nM (actual = 33 nM).

## SUMMARY AND CONCLUSIONS

To summarize, we have reported a SlipPAD for high-throughput chemical sensing in both homogeneous and heterogeneous formats. This method provides some important advantages, compared to previously reported SlipChips or  $\mu\text{PADs}$ , for certain low-cost applications. Specifically, a single individual can produce  $\sim 200$  devices per hour (Table S3 in the Supporting Information), and the cost per device is less than \$1 (Table S1 in the Supporting Information). Of course these values would improve dramatically at production scale. The total cost for the infrastructure required to produce the SlipPAD is  $\sim \$900$  (Table S2 in the Supporting Information). Moreover, the SlipPAD enables parallel delivery of liquid into an array of 285 reservoirs within seconds. Finally, the flexible and highly parallel liquid-handling capability can be harnessed for high-throughput quantitative chemical sensing with on-chip calibration and replicate measurements to improve the reliability of diagnostic results. We believe the SlipPAD is a particularly promising format for point-of-care and multiplexed assays under resource-limited conditions.

## ASSOCIATED CONTENT

### Supporting Information

Additional information as noted in text. This material is available free of charge via the Internet at <http://pubs.acs.org>.

## AUTHOR INFORMATION

### Corresponding Author

\*E-mail: [crooks@cm.utexas.edu](mailto:crooks@cm.utexas.edu). Phone: 512-475-8674.

### Present Address

<sup>†</sup>H.L.: State Key Laboratory of Bioelectronics, School of Biological Science and Medical Engineering, Southeast University, Nanjing 210096, China.

### Notes

The authors declare no competing financial interest.

## ACKNOWLEDGMENTS

We gratefully acknowledge financial support from the U.S. Defense Threat Reduction Agency (Contract Number HDTRA-1-13-1-0031). The Robert A. Welch Foundation provides sustained support for our research (Grant F-0032).

## ■ REFERENCES

- (1) Martinez, A. W.; Phillips, S. T.; Whitesides, G. M.; Carrilho, E. *Anal. Chem.* **2010**, *82*, 3–10.
- (2) Li, L.; Ismagilov, R. F. *Annu. Rev. Biophys.* **2010**, *39*, 139–158.
- (3) Pompano, R. R.; Liu, W. S.; Du, W. B.; Ismagilov, R. F. *Annu. Rev. Anal. Chem.* **2011**, *4*, 59–81.
- (4) Muller, R. H.; Clegg, D. L. *Anal. Chem.* **1949**, *21*, 1123–1125.
- (5) Lu, Y.; Shi, W. W.; Jiang, L.; Qin, J. H.; Lin, B. C. *Electrophoresis* **2009**, *30*, 1497–1500.
- (6) Carrilho, E.; Martinez, A. W.; Whitesides, G. M. *Anal. Chem.* **2009**, *81*, 7091–7095.
- (7) Li, X.; Tian, J. F.; Nguyen, T.; Shen, W. *Anal. Chem.* **2008**, *80*, 9131–9134.
- (8) Fu, E.; Lutz, B.; Kauffman, P.; Yager, P. *Lab Chip* **2010**, *10*, 918–920.
- (9) Martinez, A. W.; Phillips, S. T.; Nie, Z. H.; Cheng, C. M.; Carrilho, E.; Wiley, B. J.; Whitesides, G. M. *Lab Chip* **2010**, *10*, 2499–2504.
- (10) Liu, X. Y.; Cheng, C. M.; Martinez, A. W.; Mirica, K. A.; Li, X. J.; Phillips, S. T.; Mascarenas, M.; Whitesides, G. M. A Portable Microfluidic Paper-Based Device for ELISA. In *2011 IEEE 24th International Conference on Micro Electro Mechanical Systems*, Cancun, Mexico, January 23–27, 2011; pp 75–78.
- (11) Martinez, A. W.; Phillips, S. T.; Whitesides, G. M. *Proc. Natl. Acad. Sci. U.S.A.* **2008**, *105*, 19606–19611.
- (12) Du, W. B.; Li, L.; Nichols, K. P.; Ismagilov, R. F. *Lab Chip* **2009**, *9*, 2286–2292.
- (13) Li, L.; Du, W. B.; Ismagilov, R. F. *J. Am. Chem. Soc.* **2010**, *132*, 106–111.
- (14) Li, L.; Du, W. B.; Ismagilov, R. F. *J. Am. Chem. Soc.* **2010**, *132*, 112–119.
- (15) Shen, F.; Du, W. B.; Davydova, E. K.; Karymov, M. A.; Pandey, J.; Ismagilov, R. F. *Anal. Chem.* **2010**, *82*, 4606–4612.
- (16) Shen, F.; Du, W. B.; Kreutz, J. E.; Fok, A.; Ismagilov, R. F. *Lab Chip* **2010**, *10*, 2666–2672.
- (17) Shen, F.; Sun, B.; Kreutz, J. E.; Davydova, E. K.; Du, W. B.; Reddy, P. L.; Joseph, L. J.; Ismagilov, R. F. *J. Am. Chem. Soc.* **2011**, *133*, 17705–17712.
- (18) Liu, W. S.; Chen, D. L.; Du, W. B.; Nichols, K. P.; Ismagilov, R. F. *Anal. Chem.* **2010**, *82*, 3276–3282.
- (19) Li, L. A.; Karymov, M. A.; Nichols, K. P.; Ismagilov, R. F. *Langmuir* **2010**, *26*, 12465–12471.
- (20) Shen, F.; Davydova, E. K.; Du, W. B.; Kreutz, J. E.; Piepenburg, O.; Ismagilov, R. F. *Anal. Chem.* **2011**, *83*, 3533–3540.
- (21) Gubala, V.; Harris, L. F.; Ricco, A. J.; Tan, M. X.; Williams, D. E. *Anal. Chem.* **2012**, *84*, 487–515.
- (22) Smith, P. K.; Krohn, R. I.; Hermanson, G. T.; Mallia, A. K.; Gartner, F. H.; Provenzano, M. D.; Fujimoto, E. K.; Goeke, N. M.; Olson, B. J.; Klenk, D. C. *Anal. Biochem.* **1985**, *150*, 76–85.
- (23) Liu, H.; Crooks, R. M. *J. Am. Chem. Soc.* **2011**, *133*, 17564–17566.
- (24) Liu, H.; Xiang, Y.; Lu, Y.; Crooks, R. M. *Angew. Chem., Int. Ed.* **2012**, *51*, 6925–6928.